# An example of molecular co-evolution: Reactive oxygen species (ROS) and ROS scavenger levels in Schistosoma mansoni/Biomphalaria glabrata interactions.

Yves Moné, Anne-Cécile Ribou, Celine Cosseau, David Duval, André Théron, Guillaume Mitta, Benjamin Gourbal

# An example of molecular co-evolution: reactive oxygen species (ROS) and ROS scavenger levels in *Schistosoma mansoni/Biomphalaria glabrata* interactions

Yves Moné[a], Anne-Cécile Ribou[b], Céline Cosseau[a], David Duval[a], André Théron[a], Guillaume Mitta[a], Benjamin Gourbal[a,*]

[a] *Parasitologie Fonctionnelle et Evolutive, UMR 5244, CNRS Université de Perpignan, 52 Ave Paul Alduy, 66860 Perpignan Cedex, France*

[b] *Institut de Modélisation et d'Analyse en Géo-Environnement et Santé (laboratoire IMAGES), EA4218 Université de Perpignan, 52 Ave Paul Alduy, 66860 Perpignan Cedex, France*

*Corresponding author.

*UMR 5244, CNRS Université de Perpignan, 52 Ave Paul Alduy, 66860 Perpignan Cedex, France.*

Tel.: +33 (0)4 30 19 23 12 ; fax: 33 (0)4 68 66 22 81.

*E-mail address*: benjamin.gourbal@univ-perp.fr

**Abstract**

The co-evolution between hosts and parasites involves huge reciprocal selective pressures on both protagonists. However, relatively few reports have evaluated the impact of these reciprocal pressures on the molecular determinants at the core of the relevant interaction, such as the factors influencing parasitic virulence and host resistance. Here, we address this question in a host-parasite model that allows co-evolution to be monitored in the field: the interaction between the mollusk, *Biomphalaria glabrata*, and its trematode parasite, *Schistosoma mansoni*. Reactive oxygen species (ROS) produced by the hemocytes of *B. glabrata* are known to play a crucial role in killing *S. mansoni*. Therefore, the parasite must defend itself against oxidative damage caused by ROS using ROS scavengers in order to survive. In this context, ROS and ROS scavengers are involved in a co-evolutionary arms race, and their respective production levels by sympatric host and parasite could be expected to be closely related. Here, we test this hypothesis by comparing host oxidant and parasite antioxidant capabilities between two *S. mansoni*/*B. glabrata* populations that have co-evolved independently. As expected, our findings show a clear link between the oxidant and antioxidant levels, presumably resulting from sympatric co-evolution. We believe this work provides the first supporting evidence of the Red Queen Hypothesis of reciprocal evolution for functional traits at the field-level in a model involving a host and a eukaryotic parasite.

*Keywords*: Host-parasite co-evolution, *Schistosoma mansoni*, *Biomphalaria glabrata*, Reactive oxygen species (ROS), ROS scavengers

## 1. Introduction

Understanding the co-evolution of host-parasite interactions represents a challenge in evolutionary biology. Parasites cause substantial deleterious effects on their hosts, and therefore represent a major driving force in their evolution (Howard, 1991). Similarly, the host immune defenses represent the major selective pressure driving the evolution of parasites. For parasites to survive and develop in the host they must adapt to the host-defense system or they will die. This parallel co-evolution of host-parasite interactions can be viewed as an arms race in which both the host and the parasite develop mechanisms to circumvent the weapons developed by their opponent. In this context of reciprocal co-evolution, illustrated by Van Valen (1974), under the Red Queen Hypothesis it is assumed that the parasitic genes responsible for infectivity will evolve alongside the host defense genes, resulting in adaptation of the interactions between local host and parasite populations (Dybdahl and Storfer, 2003). To date, however, only a few studies have sought to verify this prediction and convincing experiments have only been reported for models involving viruses, bacteria and unicellular eukaryotes (Lohse et al., 2006; Forde et al., 2008).

Demonstrating co-evolution in an animal host-parasite system is not straightforward and most prior discussions of such processes have been indirect, as in studies describing local adaptation when compatibility is higher between sympatric host-parasite combinations than between allopatric combinations (Gasnier et al., 2000; Gagneux et al., 2006; Munoz-Antoli et al.), or studies that have focused on only one trait of the interaction, such as host resistance (Green et al., 2000) or parasite infectivity (Little et al., 2006). Moreover it is important to take into account that non-co-evolutionary mechanisms could also explain correlations between the traits of interacting species and that the absence of correlated traits is not evidence for an absence of co-evolution (Nuismer et al., 2007, 2010; Yoder and Nuismer, 2010). However we assume that the direct examination of reciprocal selection in both the host and the parasite could provide supporting evidence of co-evolution.

Two relatively recent studies investigated this reciprocal response more thoroughly. In the first, reciprocal changes in resistance and infectivity were identified for co-evolving *Potamopyrgus* snail hosts and their trematode parasites; however, while these changes were identified using prevalence phenotypes, they were not supported by the studied functional markers (Koskella and Lively, 2007). The second report provided experimental support for the reciprocity of adaptation costs, rapid genetic changes and increased genetic diversity during the co-evolution of a multicellular host, the nematode *Caenorhabditis elegans*, and its pathogenic bacteria, the Gram-positive bacterium, *Bacillus thuringiensis* (Schulte et al., 2010). In both papers, co-evolution was studied using laboratory strains selected by experimental evolutionary approaches, and only the second paper focused on molecular changes induced by the co-evolutionary process. Both papers were based on an "over time" approach in which the evolution of phenotypes was monitored over the course of experimental laboratory generations. Other empirical studies have been based on a "point time" approach in which the pattern of co-variations between host-parasite populations or strains that co-evolved independently were assessed at a single experimental time point (Forde et al., 2004; Morgan et al., 2005).

Here, we investigated the reciprocal evolution of molecular mechanisms directly at the core of the host-parasite interaction in a natural system of co-evolution, by comparing host and parasite populations that have co-evolved independently. As a model, we used the interaction between the trematode, *Schistosoma mansoni* (responsible for human intestinal schistosomiasis), and its mollusk intermediate host, *Biomphalaria glabrata*. This interaction is a model of choice for the study of potential co-evolutionary dynamics (Webster and Davies, 2001; Webster et al., 2004; Beltran and Boissier, 2008; Beltran et al., 2008; Bouchut et al., 2008; Roger et al., 2008a; Roger et al., 2008b; Roger et al., 2008c; Steinauer, 2009).

During its intramolluskal stage, the parasite must cope with the snail's immune system. One of the main immune effectors in mollusks are the reactive oxygen species (ROS) produced by hemocytes (the circulating immune cells of snails) (Hahn et al., 2000; de Jong-Brink et al., 2001;

95 Hahn et al., 2001b; Mourao et al., 2009b). Previous studies conducted by Hahn and co-workers
96 demonstrated that hydrogen peroxide ($H_2O_2$) plays a crucial role in the killing of *S. mansoni*
97 sporocysts (Hahn et al., 2001a, b). Furthermore, hemocytes from *S. mansoni*-resistant snails were
98 shown to generate significantly more $H_2O_2$ than susceptible snails, perhaps due at least in part to the
99 former having constitutively elevated levels of the mRNA encoding the copper/zinc superoxide
100 dismutase (Cu-ZN SOD) (Goodall et al., 2004; Bender et al., 2005; Bender et al., 2007). To resist
101 ROS-mediated attacks, the *S. mansoni* larvae produce ROS-detoxifying enzymes (Vermeire et al.,
102 2006; Guillou et al., 2007; Vermeire and Yoshino, 2007; Roger et al., 2008c; Wu et al., 2009),
103 several of which appear to be secreted by sporocysts (Guillou et al., 2007; Wu et al., 2009).
104 Supporting this, a recent report showed that antioxidant enzymes produced by *S. mansoni*
105 sporocysts are directly involved in protecting the pathogen against immune cell-mediated oxidative
106 stress (Mourao et al., 2009b).

107 In this context, the snail-produced ROS and the parasite-produced ROS scavengers are
108 involved in a co-evolutionary arms race, and we can hypothesize that their production levels will be
109 closely related. Here, we tested this hypothesis by comparing host oxidant and parasite antioxidant
110 abilities for two *S. mansoni*/*B. glabrata* strains that have evolved independently, originated from
111 different geographic endemic zones and which are found to display significant differences in
112 compatibility.

113

114 **2. Materials and methods**

115 *2.1 Ethics statement*

116 Our laboratory has received the permit # A66040 for experiments on animals from both the French
117 Ministry of agriculture and Fishing and the French Ministry of National Education, Research and
118 Technology. Housing, breeding and animal care of the mice followed the ethical requirements of
119 French government. The experimenter possesses the official certificate for animal experimentation

delivered by both ministries (Décret # 87–848 du 19 octobre 1987; number of the authorization 007083).

### *2.2. Biological materials*

Two strains of *S. mansoni* were used in this study: a Brazilian strain (*Sm*BRE) and a Guadeloupean strain (*Sm*GH2). Each strain was maintained: (i) in their sympatric strain of *B. glabrata* (*Bg*BRE and *Bg*GUA, respectively); and (ii) in hamsters (*Mesocricetus auratus*), as described previously (Théron et al., 1997).

Miracidia from *Sm*BRE and *Sm*GH2 were hatched from eggs axenically recovered from 60-day-infected hamster livers, according to the previously described procedure (Roger et al., 2008c). Briefly, livers were collected and kept overnight at 4°C in sterile saline solution (NaCl 150 mM) containing an antibiotic/antimycotic mixture (penicillin 100 units/ml, streptomycin 0.1 mg/ml, amphotericin B 0.25 µg/ml; Sigma). The livers were then homogenized and the eggs were filtered out, washed, and transferred to spring water. The miracidia were allowed to hatch out under illumination.

### *2.3. Schistosome-snail compatibility: snail exposure, infection rates and intensities*

The compatibilities of the tested snail-schistosome combinations were evaluated by monitoring the infection rates (% of snails infected) and the intensity of infection (number of mother sporocysts (SpI) developed) among snails individually challenged with different numbers of miracidia. As the miracidial dose increased, a larger fraction of the phenotypic diversity in the parasitic isolate was sampled; thus, dose-response curves are much more informative than single-dose challenges when examining the dynamics of compatibility between two host-parasite combinations (Théron et al., 2008).

For each experiment, snails (7-9 mm in diameter) were exposed individually to a fixed number of miracidia in approximately 10 ml of water for 8 h. Following exposure to miracidia, the

146 snails were replaced in their original containers until their infection status (presence of SpI) was
147 assessed. For the detection of SpI, the snails were fixed 15 days post-exposure, following
148 previously described methods (Gerard et al., 1995; Moné et al., 2010b). In brief, each snail was
149 relaxed in pond water containing an excess of crystalline menthol for 6 h, the body was removed
150 and fixed in modified Raillet-Henry's solution, exhaustive dissection of the head-foot zone was
151 performed, and the number of SpI present in each snail (readily observable as translucent white
152 bodies within an opaque gray tissue background) was determined.

153 Dose-response curves were obtained by challenging individual snails (30-40 snails per
154 treatment) with doses of 1, 10, 20, 30 and 50 miracidia. Compatibility was measured for the two
155 sympatric combinations (*Sm*BRE versus *Bg*BRE and *Sm*GH2 versus *Bg*GUA) and the two
156 allopatric combinations (*Sm*BRE versus *Bg*GUA and *Sm*GH2 versus *Bg*BRE).

157

158 *2.4. Cytotoxicity of $H_2O_2$ on S. mansoni sporocysts*

159 $H_2O_2$ cytotoxicity was measured using the Roche Cytotoxicity Detection Kit (Roche
160 Diagnostics, Mannheim, Germany), which is based on the measurement of lactate dehydrogenase
161 (LDH) activity released from dead and lysed cells into the supernatant. Four hundred miracidia each
162 of *Sm*BRE and *Sm*GH2 were submitted to in vitro transformation to obtain primary sporocysts
163 (Sp1). Briefly, the miracidia were cultured for 24 h in sterile Chernin's balanced salt solution
164 (CBSS) (Chernin, 1963), containing an antibiotic/antimycotic mixture (penicillin 100 units/ml,
165 streptomycin 0.1 mg/ml, amphotericin B 0.25 µg/ml; Sigma). The sporocysts were then exposed to
166 four different concentrations of $H_2O_2$ (0, 75, 150 and 200 µM) for 2 h and cytotoxicity was
167 examined according to the manufacturer's instructions. As a positive control, we measured LDH
168 release from Sp1 that had been lysed with the provided lysis solution (high control, HC); this was
169 taken as 100% LDH release. To correct for the background, we measured LDH levels in Sp1-free
170 $H_2O_2$-treated culture medium (substance control, SC). All measured values were assayed in

triplicate. The percentage of specific $H_2O_2$-induced LDH release was determined as: % cytotoxicity = [(experimental result - SC)/(HC - SC)] x 100.

*2.5. Effect of $H_2O_2$ on S. mansoni sporocyst mortality*

Two independent experiments were conducted in triplicate on 24-well plates containing 20 Sp1 (representing *Sm*BRE or *Sm*GH2) per well. The Sp1 were in-vitro transformed as described above (see Materials and methods section 2.2), and exposed to 0, 200, 400, 800 or 1,600 µM of $H_2O_2$ (Hydrogen peroxide 35%, FLUKA, Germany) for 4 h. Mortality was assessed under a light microscope, with the Sp1 considered "dead" when we failed to observe motility and/or the beating of the flame-cell flagella.

*2.6. The total antioxidant capacity of S. mansoni sporocysts*

The cumulative (total) antioxidant capacity of the sporocysts was quantified for the two parasite strains, *Sm*BRE and *Sm*GH2, using an Antioxidant Assay Kit (Sigma). For each test, 2,000 sporocysts were in-vitro transformed as described above. After 24 h, fully transformed sporocysts were recovered by gentle centrifugation (800 *g*, 5 min, 4°C). The samples were then disrupted by sonication (three pulses of 20 s each) and pelleted by centrifugation (12,000 *g*, 15 min, 4°C), and the antioxidant capacity of each supernatant was determined following the manufacturer's recommendations. The amount of protein in each supernatant was determined using a Bradford protein assay kit and used as a correcting factor. The experiment was performed six times per strain.

*2.7. Reverse Transcription-quantitative PCR (RT-qPCR)*

*RT-qPCR* analyses were conducted to compare the expression of parasite antioxidant enzymes suspected to play key roles in the detoxification of host-induced oxidative stress. Real-time PCR analyses were performed using a LightCycler 2.0 system (Roche Applied Science) and a LightCycler Faststart DNA Master SYBR Green I kit (Roche Applied Science). Total RNA extractions from miracidia were performed using the Trizol Reagent (Life Technologies, USA) and

198 the manufacturer's protocol. Reverse transcription was performed according to previously described
199 procedures (Guillou et al., 2004). qPCR amplification was performed using 2.5 µl of cDNA in a
200 final volume of 10 µl containing 3 mM $MgCl_2$, 0.5 µM of each primer and 1 µl of master mix. The
201 primers were designed using either the LightCycler probe design software or the web-based
202 Primer3 plus interface (http://www.bioinformatics.nl/cgibin/ primer3plus/primer3plus.cgi) and are
203 given in Table 1. The following Light-Cycler run protocol was used: denaturation at 95◦C for 10
204 min, followed by 40 cycles of amplification and quantification at 95◦C for 10 s, 60◦C for 5 s and
205 72◦C for 16 s, a melting curve of 60–95◦C with a heating rate of 0.1◦C/s and continuous
206 fluorescence measurement, and then a cooling step to 40◦C. For each reaction, the cycle threshold
207 (Ct) was determined using the "Fit Point Method" of the LightCycler Software, version 3.3. The
208 PCR reactions were performed in duplicate and the mean Ct value was calculated. For each sample,
209 the expression level of the target gene was normalized with regard to the expression of two
210 constitutively expressed genes (28S rRNA and α tubulin). The expression ratio (R) was calculated
211 according to the formula: $R = 2(\Delta Ct)$, where ΔCt represents Ct (target gene) – Ct (constitutively
212 expressed gene).
213
214 *2.8. ROS detection in single cells*
215 The cell-permeable fluorescent oxygen probe, 1-pyrenebutyric acid (PBA), can be used for
216 the measurement of free radicals in solution (Oter and Ribou, 2009) and in living cells (Ribou et al.,
217 2004; Rharass et al., 2006), with the fluorescence intensity and lifetime of PBA decreasing
218 proportionately to the free-radical concentration. Measurement of the fluorescent lifetime offers
219 many advantages over intensity based measurements when working in vivo, not the least that the
220 measurements are independent of the absolute intensity of emitted light and the fluorophore
221 concentration, thereby avoiding artifacts arising from optical losses. Moreover, these probes do not
222 require a reaction with ROS, are usually stable and the fluorescent lifetime is not modified by probe
223 degradation or variations in its intracellular accumulation.

224

225 *2.8.1. Staining and fixation*

226 Hemolymph samples were recovered from *Bg*BRE and *Bg*GUA snails, and aliquots (150 µl)
227 were put in a Sykes-Moore chamber. After 4 h, the adhered hemocytes were rinsed with Hank's
228 buffered salt solution (HBSS) and stained for 20 min with PBA (Acros Organics, Belgium; 0.10
229 µM in 1% ethanol). The hemocytes were then rinsed three times and placed in HBSS for
230 measurements. For fixation experiments, hemocytes were treated as described above except that
231 after the final rinsing step, the cells were killed by incubation for 10 min in Baker solution (10%
232 paraformaldehyde in 1% aqueous calcium chloride). In the latter case, the experiments were
233 performed within 1 h after cell killing, in order to avoid probe reorganization (Ribou et al., 2004).

234

235 *2.8.2. ROS quantification by fluorescent-lifetime measurement of single cells*

236 The fluorescent decay of single living cells loaded with PBA was recorded using time-
237 resolved microfluorimetry, as previously described (Ribou et al., 2003). Briefly, a laser (nitrogen
238 laser NL100; Stanford Research Systems, USA) delivered monochromatic 337-nm pulses, each
239 with a half-amplitude pulse-width of 3 ns, and an objective (40×; Unitron) was used to concentrate
240 the excitation beam on the microscopic sample. Emitted photons were collected and focused on a
241 photomultiplier 1P28 (Hamamatsu Corporation, Japan). A diaphragm placed on the emission
242 pathway allowed the selection of signals from single cells, while a 404-nm bandpass filter (half
243 bandwidth; 40 nm) also located along the emission pathway was used to select the pyrene emission.
244 Each signal was digitalized by a digital oscilloscope (TDS 3032C; Tektronix, USA). The
245 fluorescent decay of single PBA-loaded cells selected by the 404-nm filter could be resolved into
246 three exponential curves. The time constants (i.e. lifetimes) and amplitude values of each
247 exponential curve in the decay were obtained using the downhill simplex method (Nelder and
248 Mead, 1965). The first two decays corresponded to the intrinsic fluorescence of the cell attributed to
249 the reduced form of NAD(P)H. The third long-time constant (> 100 ns), which was characteristic of

pyrene derivatives, was related to the ROS concentration through the Stern-Volmer equation (Stern and Volmer, 1919) that describes collisional fluorescent quenching of a probe (i.e. PBA) by a quencher (i.e., free radicals). The method has been described in several papers (Ribou et al., 2003; Ribou et al., 2004; Rharass et al., 2006). We calculated the variation of intracellular ROS concentrations as follows:

$$[ROS] / [ROS]_m = [t_m (t_0 - t)] / [t(t_0 - t_m)] \quad \text{Equation 1}$$

where t is the fluorescent lifetime measured for 108 single hemocytes originating from eight *Bg*BRE snails and 111 cells from eight *Bg*GUA snails; $t_m$ is the mean of all lifetimes; and $t_0$ is the fluorescent lifetime in the absence of ROS (measured from dead hemocytes fixed with Baker solution). In this equation, $[ROS]_m$ is the mean of the concentrations from all tested cells (219 cells). We assumed that fixation ended all cellular activity and ROS production. In the presented data, the mean ROS concentration has been assigned an arbitrary value of 1.

### *2.9. $H_2O_2$ production and release by B. glabrata hemocytes*

The $H_2O_2$ production by hemocytes was measured using Amplex® Red (Invitrogen). Hemolymph was collected from the head-foot regions of *Bg*BRE and *Bg*GUA snails (7-11 mm in diameter) as previously described (Bouchut et al., 2006), and the number of hemocytes per µl of hemolymph was quantified using a cell counter (Z Series Coulter Counter; Beckman Coulter); 226.2 ± 50.6 cells /µl and 241.2 ± 102.1 cells /µl were obtained for *Bg*BRE and *Bg*GUA, respectively. The Hemolymph of four snails was pooled and 45,000 hemocytes per well were dispensed to a 96-well plate for each strain. The hemocytes were allowed to adhere and spread for 1 h at 26°C. The plate was then centrifuged (600g for 10 min), the plasma was removed, the adhered hemocytes were washed three times with HBSS, and the wells were treated with Amplex® Red reaction mixture (100 µL per well, prepared according to the manufacturer's instructions). Optical density was measured with a microplate reader at 570 nm during the following 1 h (at 5, 10, 15, 20, 30, 40, 50, 60 min). The results are expressed as Amplex Red O.D. at 570 nm / 45,000 cells.

### *2.10. Biomphalaria glabrata superoxide anion plasma content*

The plasma content of superoxide anion was monitored via the superoxide-mediated reduction of nitroblue tetrazolium (NBT), which results in the precipitation of an insoluble blue formazan that can be quantified spectrophotometrically. Briefly, hemolymph was collected from *Bg*BRE and *Bg*GUA snails as described above. Hemocytes were removed by centrifugation (1,500 *g* for 15 min), and then 50 µL of plasma from each snail was mixed with 50 µl of 0.1% NBT (Sigma) dissolved in PBS; ($Na_2HPO_4$ 8.41 mM, $NaH_2PO_4$ 1.65 mM, NaCl 45.34 mM, pH 7.45). Formazan blue formation was measured with a microplate reader at 620 nm over the course of 3 h (at 5, 10, 15, 30, 60, 90, 180 min). NBT-free plasma was used as a control, and triplicate experiments were conducted for 10 individuals per strain.

### *2.11. Statistical analyses*

The normality of our experimental data was assessed using the Shapiro-Wilk normality test (Shapiro and Wilk, 1965). Our data on the effect of $H_2O_2$ cytotoxicity on *S. mansoni* sporocysts (LDH test), *B. glabrata* hemocyte $H_2O_2$ production, and superoxide anion plasma content were all found to be normally distributed ($P > 0.05$), and were subsequently analyzed using the student's *t*-test. Our data on the effect of $H_2O_2$ on *S. mansoni* sporocyst mortality and the total antioxidant capacity of sporocysts were not normally distributed ($P < 0.05$), and were subsequently analyzed using the Mann-Whitney test. The results of the ROS concentration assays in each mollusk strain were analyzed using the Mann-Whitney test. The Kolmogorov-Smirnov two-samples test was utilized to determine whether the ROS concentrations were similarly distributed in hemocytes from *Bg*BRE and *Bg*GUA.

## 3. Results

### *3.1. Effect of $H_2O_2$ on S. mansoni sporocysts*

Two different assays were conducted to test the effect of $H_2O_2$ on the two strains of *S. mansoni* sporocysts (*Sm*BRE and *Sm*GH2) (Fig. 1). First, an LDH test was used to examine the cytotoxicity of $H_2O_2$ on sporocysts of each strain. Our results revealed that the susceptibility to $H_2O_2$ was significantly higher for SmGH2 than *Sm*BRE (Fig. 1A). When exposed to 200 μM $H_2O_2$, *Sm*GH2 sporocysts showed 25.8% cytotoxicity (i.e., 25.8% of the cells had lysed and released their LDH content), whereas no changes were observed for *Sm*BRE at the same $H_2O_2$ concentration (Fig. 1A). However, although cell lysis occurred in *Sm*GH2, the sporocysts were still alive at this concentration. To investigate possible between-strain differences in mortality, we next exposed sporocytes to increasing concentrations of $H_2O_2$ and examined motility and the beating of the flame-cell flagella, which were taken as distinguishing between living and dead larvae. No difference between the two strains was observed until the concentration of $H_2O_2$ reached 1,600 μM (Fig. 1B). At this concentration, 31.2% and 2.6% of the *Sm*GH2 and *Sm*BRE sporocysts were dead, respectively; this difference is statistically significant (student's *t*-test; $P = 0.017$). These results suggest that *Sm*GH2 sporocysts are more susceptible to $H_2O_2$ than *Sm*BRE sporocysts.

### *3.2. The total antioxidant capacity of S. mansoni sporocysts*

To investigate potential differences in the constitutive antioxidant abilities of sporocysts from *Sm*BRE and *Sm*GH2, we measured the cumulative antioxidant activities of these two strains (Fig. 2). Our results revealed that the antioxidant ability of *Sm*GH2 was significantly lower than that of *Sm*BRE (approximately 13% less; Mann-Whitney test, $P = 0.0001$).

### *3.3. Reverse Transcription-quantitative PCR of ROS-scavenger expression among S. mansoni strains*

RT-qPCR was used to compare the expression of parasite antioxidant enzymes suspected to play key roles in the detoxification of host-induced oxidative stress (Table 1) (Guillou et al., 2007). Notably, Cu-Zn SOD (Smp_176200.2) was found to be expressed at a significantly higher level in

328 *Sm*BRE than in *Sm*GH2 (2.7-fold; $P = 0.017$) (Fig. 3). In contrast, no difference was observed in the
329 expression levels of glyceraldehyde-3-phosphate dehydrogenase (GAPDH, Smp_056970.1), GST
330 omega (Smp_152710.1), GST 28 kD (Smp_054160), GST 26 kD (Smp_163610), glyoxalase II
331 (Smp_091010) or thioredoxin peroxidase (TPX, Smp_158110) (data not shown).
332
333 *3.4. Intracellular ROS measurements in single B. glabrata hemocytes*
334 We monitored intracellular ROS levels in single hemocytes, using PBA. This method allows
335 global ROS to be measured without interference from the reactive hydroxyl radical or $H_2O_2$. PBA
336 fluorescent lifetimes were measured for 108 and 111 individual hemocytes originating from eight
337 *Bg*BRE and eight *Bg*GUA snails, respectively. *Bg*BRE hemocytes produced significantly (11.2%)
338 more ROS than *Bg*GUA hemocytes (Mann-Whitney test; $P = 0.009$) (Fig. 4A). Fig. 4B shows the
339 distribution of hemocytes from both strains according to their ROS concentrations, which were
340 calculated from the ratio given in equation 1 (see Materials and methods section *2.8.2.*). Although
341 the cells from both *Bg*BRE and *Bg*GUA samples were distributed around the mean ROS
342 concentration, their distributions were significantly different (Kolmogorov-Smirnov test, $P =$
343 0.012). Among the hemocytes producing more than 1.5-fold of the mean ROS concentration, 68.8%
344 were from *Bg*BRE strain, while only 31.2% were from *Bg*GUA. Conversely, among the hemocytes
345 that showed the lowest ROS concentrations (< 0.7-fold of the mean ROS concentration) 38.1%
346 were from *Bg*BRE and 62% were from *Bg*GUA (Fig. 4B). By recording the fluorescent lifetimes of
347 single cells loaded with PBA, we also obtained the relative concentrations of free and bound
348 NAD(P)H (an indicator of metabolic change) in each cell. However there was no significant
349 difference in the quantity of bound and free NAD(P)H (mean ratio = 0.60 for both strains; data not
350 shown), suggesting that the strains had similar levels of metabolism. Thus, the only molecular
351 difference observed between the two strains was the level of ROS production.
352
353 *3.5. $H_2O_2$ production and release by B. glabrata hemocytes*

We assessed $H_2O_2$ production and secretion by hemocytes of both strains using Amplex Red. Fig. 5 shows the cumulative amount of $H_2O_2$ constitutively released by hemocytes of each strain over 1 h. The maximum level of $H_2O_2$ production was reached at 20 min for *Bg*GUA and at 40 min for *Bg*BRE after addition of Amplex Red substrate. In total, *Bg*BRE hemocytes produced significantly more (1.44-fold; mean value) $H_2O_2$ than *Bg*GUA hemocytes (student's *t*-test; $P < 0.05$) (Fig. 5).

### *3.6. Biomphalaria glabrata superoxide anion plasma content*

To our knowledge, all spectrophotometric methods currently available for the determination of $H_2O_2$ are based on the measurement of red or orange pigments, making these methods unsuitable for use on *B. glabrata* plasma samples, which are already tinted red by hemoglobin. Consequently, we used NBT to measure the amount of superoxide anion ($O_2^{\cdot-}$; a precursor of $H_2O_2$) produced in both strains. As shown in Fig. 6, at 3 h after addition of NBT *Bg*BRE plasma contained significantly more (44% more) superoxide anion than *Bg*GUA plasma (student's *t*-test; $P = 0.0007$).

### *3.7. Compatibility of sympatric and allopatric S. mansoni/B. glabrata combinations*

Sympatric pairings of *S. mansoni* and *B. glabrata* originating from Brazil and Guadeloupe were previously shown to display different levels of compatibility that remained remarkably stable across laboratory generations (Théron et al., 2008). We first used dose-response curves obtained by challenging snails with increasing doses of miracidia to confirm that similar differences could be observed between our strains. At doses of 10 or more miracidia/snail, *Sm*BRE/*Bg*BRE showed an infection rate of 100%, while *Sm*GH2/*Bg*GUA had an infection rate of approximately half that, at around 55%. Interestingly, differences were also observed for the number of parasites (SpI) that develop within the snails. The infection intensity rose gradually as the challenge doses increased for *Sm*BRE/*Bg*BRE, reaching 16.18 ± 0.86 parasites/snail at the 50-miracidia dose. In contrast, the

infection intensity for *Sm*GH2/*Bg*GUA remained low regardless of the challenge dose, varying between 1.6 ± 0.20 and 3.2 ± 0.64 parasites/snail (Fig. 7).

When we tested the heterologous combinations, we found that the *Sm*BRE/*Bg*GUA pairing showed a substantial level of compatibility, with infection rates of 80-90% (not significantly different from the 100% achieved by the *Sm*BRE/*Bg*BRE pairing), but with lower parasite intensities (9.8 ± 0.89 for the 50-miracidia dose) compared with the sympatric combination (16.18 ± 0.86 parasites/snail at the 50-miracidia dose). In contrast, the *Sm*GH2/*Bg*BRE combination showed very little infectivity, with infection rates < 6% and ~1 parasite/snail regardless of the challenge dose (Fig. 7).

### *3.8. ROS, ROS scavengers and compatibility in sympatric and allopatric S. mansoni/B. glabrata combinations*

The above-described results indicated that levels of ROS and ROS scavengers were correlated in both sympatric combinations, with high-level ROS/ROS scavenger production in the Brazilian combination, but lower-level ROS/ROS scavenger production in the Guadeloupean combination. If high levels of *S. mansoni* ROS scavenger are correlated with better resistance of the intramolluskan stage of the parasite (as we hypothesized), we would expect *Sm*GH2 to have a relatively low ability to infect the allopatric *Bg*BRE snails, while *Sm*BRE would have a high ability to infect the allopatric *Bg*GUA snails. This hypothesis was verified in our model, as shown in Fig. 8.

## 4. Discussion

Snail-schistosome compatibility and infection rates result from a complex interplay between the host's defense mechanisms and the parasite's infectivity strategies. Due to selective pressures exerted by the parasite on the host and vice versa, co-evolutionary dynamics may be observed (Janzen, 1980; Howard, 1991). Between-population or between-strain differences in the outcomes

405 of such evolutionary processes may be expected due to differences in the epidemiological and
406 environmental conditions, and/or genetic architectures. Such differential selection patterns could
407 explain, at least in part, the geographic and/or strain-specific compatibility variations seen in snail-
408 schistosome interactions (Théron et al., 2008). At present, however, there is relatively little
409 empirical evidence demonstrating reciprocal molecular adaptations in both host and parasite.

410 Here, we investigated the interaction between *S. mansoni* and the snail, *B. glabrata*, as this
411 interaction is a popular model for the study of co-evolutionary dynamics (Beltran and Boissier,
412 2008; Beltran et al., 2008; Bouchut et al., 2008; Roger et al., 2008a; Roger et al., 2008b; Roger et
413 al., 2008c; Steinauer, 2009). We confirmed that there are different levels of compatibility between
414 two geographic strains of *S. mansoni* and their sympatric snail hosts, *B. glabrata* (Fig. 7) that both
415 have co-evolved independently. We compared the host oxidant and parasite antioxidant abilities
416 that appear to form the core of the attack/defense interactions of these two pairings.

417 ROS are the main effectors of the snail immune system; they are highly reactive and can
418 trigger irreversible cell damage. Indeed, ROS produced by the hemocytes of *B. glabrata* are known
419 to play a crucial role in the killing of *S. mansoni* (Hahn et al., 2000; Hahn et al., 2001a, b; Bender et
420 al., 2005; Bayne, 2009). Conversely, *S. mansoni* possess antioxidant systems capable of
421 counteracting the ROS produced by their host's immune system. *Schistosoma mansoni* is exposed
422 to ROS in both their intermediate (snail) and definitive (human or mammalian) hosts, and produce
423 oxidative-stress scavengers in their excretory-secretory products (ESP) during all stages of their life
424 cycle (Mei and LoVerde, 1997; Curwen et al., 2004; Zelck and Von Janowsky, 2004; Knudsen et
425 al., 2005; van Balkom et al., 2005; Bernal et al., 2006; Dzik, 2006; Perez-Sanchez et al., 2006; Cass
426 et al., 2007; Guillou et al., 2007; Mourao et al., 2009a; Wu et al., 2009). Therefore, the success or
427 failure of host invasion by *S. mansoni* depends at least in part on its ability to defend itself against
428 oxidative damage (Mourao et al., 2009a). In this system, therefore, ROS and ROS scavengers
429 should be involved in a co-evolutionary arms race, and we would expect their respective production
430 levels in sympatric host/parasite combinations to be closely related.

As previous studies have established that $H_2O_2$ is the main ROS involved in killing *S. mansoni* sporocysts, probably due to its stability and capacity to cross cell membranes (Hahn et al., 2001b; Bienert et al., 2006), we studied the susceptibility of two strains of *S. mansoni* to $H_2O_2$. Our results showed a clear intrinsic difference between parasites isolated from two different geographic regions: the intramolluskan stages of Guadeloupean *S. mansoni* (*Sm*GH2) were more sensitive to $H_2O_2$ than those of the Brazilian strain (*Sm*BRE) (Fig. 1). Moreover, we observed a difference in antioxidant potential between strains, with *Sm*GH2 displaying a lower level of antioxidant activity than *Sm*BRE (Fig. 2). Thus, *Sm*BRE has a more efficient antioxidant system, which would seem to explain its higher level of resistance to $H_2O_2$-mediated oxidative damage.

In order to identify the molecular pathways involved in these differential antioxidant properties, we investigated the strain-specific transcription levels of genes encoding various antioxidant enzymes, including GAPDH (Smp_056970.1), GST omega (Smp_152710.1), GST28 (Smp_054160), GST26 (Smp_163610), glyoxalase II (Smp_091010), thioredoxin peroxidase, and Cu-Zn SOD (Smp_176200.2) (Guillou et al., 2007; Vermeire and Yoshino, 2007; Roger et al., 2008c; Mourao et al., 2009a; Wu et al., 2009). Among these candidates, only the Cu-Zn SOD mRNA displayed differential expression, with expression levels that were 2.7-fold higher in *Sm*BRE than in *Sm*GH2 (Fig. 3). This finding is consistent with our protein-level results from a previous proteomic study (Roger et al., 2008c), and these observations collectively suggest that Cu-Zn SOD plays a key role in the antioxidant strategy of *S. mansoni*. The involvement of Cu-Zn SOD in ROS detoxification is a recurring and intriguing question, because it is capable of dismutating the superoxide anion ($O_2^{\bullet-}$) to produce $H_2O_2$ (Zelck and Von Janowsky, 2004; Guillou et al., 2007; Mourao et al., 2009a). The hypothesis currently used to explain the role of *S. mansoni* Cu-Zn SOD in ROS detoxification is based on a suspected peroxidative function (Yim et al., 1993; Yim et al., 1996; Kim and Kang, 1997; Bayne et al., 2001). In short, it has been proposed that *S. mansoni* Cu-Zn SOD could use its own dismutation product ($H_2O_2$) to produce hydroxyl radicals ($HO^{\bullet}$) that are less toxic for sporocysts (Bayne et al., 2001).

In a co-evolutionary context, the between-strain differences in ROS susceptibility and antioxidant activity of these *S. mansoni* strains suggest that there could be comparable differences in the ROS production capabilities of the host snail strains. To test this hypothesis, we investigated ROS production by the two snail strains. First, we used a fluorescence-based method (Rharass et al., 2006) to investigate the hemocyte production of free-radicals such as nitric oxide and superoxide anion. This approach revealed that *Bg*BRE snails produced more free radicals than *Bg*GUA snails (Fig. 4A). Moreover, a distribution analysis of free-radical concentrations in single hemocytes showed that the cells producing higher concentrations of ROS came from *Bg*BRE individuals, while those producing lower levels of free radicals were from *Bg*GUA snails (Fig. 4B).

However, although our results revealed that global ROS production differed between BgBRE and BgGUA, oxidants can differ in their reactivity and efficient parasite killing requires that the host produce the right oxidant (Bayne et al., 2001). As previous studies have demonstrated the crucial role of hydrogen peroxide ($H_2O_2$) in the killing of *S. mansoni* sporocysts (Hahn et al., 2001b; Goodall et al., 2004; Bender et al., 2005; Bender et al., 2007), we investigated potential differences in hemocyte $H_2O_2$ production between the snail strains. Our results showed that hemocytes from *Bg*BRE constitutively produced more $H_2O_2$ than those from *Bg*GUA (Fig. 5). We then examined the $H_2O_2$ content of plasma from these snails. As technical restrictions make it impossible to directly measure $H_2O_2$ in plasma, we measured the superoxide anion, which is a precursor of $H_2O_2$ (Selkirk et al., 1998). Our results confirmed that *Bg*BRE plasma contained significantly more superoxide anion than *Bg*GUA plasma (Fig. 6). All of these data were obtained from hemocytes harvested from uninfected snails and without cell stimulation. Notably, no difference in ROS production was observed when these hemocytes were stimulated by the addition of phorbol 12-myristate 13-acetate (PMA) to culture medium (data not shown).

Taken together, our data show that: (i) the production of ROS in general and $H_2O_2$ (the main ROS acting against *S. mansoni* sporocysts) in particular differ between the two snail strains; and (ii) this $H_2O_2$ production seems to be correlated with the level of ROS scavengers produced by

483 sympatric parasites. *Bg*BRE snails produce higher amounts of $H_2O_2$ and interact naturally with
484 *Sm*BRE, which have better resistance against oxidative stress, while *Bg*GUA snails produce less
485 $H_2O_2$ and are sympatric with *Sm*GH2, which is more susceptible to ROS. If our hypothesis is
486 accurate, therefore, we would expect our cross-infection experiments to reveal differences: (i) in the
487 infective potential of our two *S. mansoni* strains; and (ii) in the resistance potential of our two *B.*
488 *glabrata* strains.

489 Indeed, the results of the infection and cross-infection experiments showed significant
490 differences in the infection rates and intensities (Fig. 7). The factors and mechanisms underlying
491 these differences are not yet known, but may include historical epidemiological conditions,
492 differential selective pressures in the transmission areas, genotypic diversities in the host and
493 parasitic isolates, recognition mechanisms developed through the matching-phenotypes model, and
494 intraspecific competition among sporocysts (for details, see (Théron et al., 1997; Théron and
495 Coustau, 2005; Théron et al., 2008; Bech et al.). Notably, the host-parasite combination
496 characterized by the higher infection rates and parasite intensities (*Sm*BRE/*Bg*BRE) was also
497 characterized by a higher ROS-production capacity by the host and a higher ROS-scavenging
498 ability by the parasite. In contrast, the host-parasite combination with lower infection rates and
499 parasite intensities (*Sm*GH2/*Bg*GUA) showed lower ROS production by the host and lower ROS
500 scavenging by the parasite (Fig. 8). These observations argue for the presence of reciprocal
501 adaptation between the ROS and ROS scavenger traits. This was further supported by the results
502 from our allopatric cross-infections. The *Sm*GH2 strain, which had co-evolved with its sympatric
503 snail (*Bg*GUA) to produce lower levels of ROS, could not effectively infect high-ROS-producing
504 *Bg*BRE snails (Figs. 7 and 8). Conversely, the *Sm*BRE strain, which had co-evolved with a host that
505 produced more ROS (*Bg*BRE), could easily infect low-ROS-producing *Bg*GUA snails (Figs. 7 and
506 8). Interestingly, however, the infection success of *Sm*BRE was lower for the allopatric combination
507 than the sympatric pairing (Figs. 7 and 8), suggesting that the oxidative factors probably act in
508 combination with other factors to determine the outcome of the *B. glabrata*/*S. mansoni* interaction.

509 Within hosts, immune effectors exert the main selective pressure on parasites (Loker and
510 Adema, 1995; Damian, 1997). However, another factor that helps to define the interaction is the
511 efficiency of parasite recognition by snail immune receptors, and the ability of the parasite to escape
512 this recognition. We previously discovered a group of polymorphic antigens of *S. mansoni* (the *S.*
513 *mansoni* polymorphic mucins, *Sm*PoMucs) (Roger et al., 2008a; Roger et al., 2008b; Roger et al.,
514 2008c), and recently showed that these antigens are recognized by diversified *B. glabrata* immune
515 receptors (the fibrinogen-related proteins, FREPs) (Moné et al., 2010a). These reports on the
516 molecular interactions underlying snail-schistosome compatibility suggest that co-evolutionary
517 (reciprocal adaptation) processes probably occur through a combination of changes in general
518 resistance (ROS/ROS scavengers) and more specific interactions (FREPs/*Sm*PoMucs). In non-
519 specific resistance/infectivity interactions involving density-dependant forces (e.g., the number of
520 developing parasites within the host), co-evolution leads to global increases in the amount of
521 attack/defense products, such as the interplay of ROS and ROS scavengers described herein. In
522 highly specific genotype-by-genotype interactions, such as recognition/evasion processes, however,
523 co-evolution leads to increases in the diversification and/or polymorphisms among specific
524 molecules, as observed for FREPs and *Sm*PoMucs.
525 Even if the success of infection is not exclusively based on the levels of ROS and ROS
526 scavengers, our model of dynamic co-evolution predicts that a change in parasite virulence or host
527 resistance would be associated with life history trade-offs (reallocation of resources), with increased
528 production of a molecule under co-evolutionary pressure yielding indirect negative consequences
529 for other functions (development, growth, fecundity, reproductive rate, etc.) (Green et al., 2000;
530 Lohse et al., 2006; Forde et al., 2008). Indeed, this kind of trade-off has been observed in our
531 model, as a previous study showed that cumulative cercarial production was two-fold higher for the
532 *Sm*GH2/*Bg*GUA combination than for the *Sm*BRE/*Bg*BRE (Théron et al., 1997). This could
533 indicate that *Sm*BRE has made a tradeoff by investing in the production of ROS scavengers at the
534 expense of producing cercariae.

In summary, host-parasite interactions are dynamic biological systems in which the host's defense mechanisms face the parasite's infectivity mechanisms, leading to a co-evolutionary arms race (Combes, 2000; Howard and Jack, 2007).

Developing correlation approaches to studying co-evolution have some limitations. Indeed the correlations between traits of interacting species cannot always provide unequivocal evidence for co-evolution. Reciprocity could also occur and an absence of correlated traits is not evidence for an absence of co-evolution (Nuismer et al., 2007; Nuismer et al., 2010; Yoder and Nuismer, 2010). Non-co-evolutionary mechanisms could explain correlations between the traits of interacting species. For example, the correlation could result from a colonization process in which a parasite species with new potential arrived in a new environment and is more well-adapted to the sympatric interacting species. In other interaction models correlated traits could evolve if the abiotic or biotic environments favour similar traits in both of the interacting species. For example, a biotic selection that affects only one of the interacting species can itself cause trait matching. This can occur if interactions have potent fitness consequences for only one of the species or if the outcome of interactions depends on the phenotype of only one of the species. These one-way interactions can generate correlations that are indistinguishable from those that evolve due to co-evolutionary processes (Nuismer et al., 2007; Nuismer et al., 2010; Yoder and Nuismer, 2010). In our model of interest *B. glabrata* could be infected by a lot of pathogens species (other than *S. mansoni*) that represent a selective pressure that could enhance snail ROS production. In this context, schistosomes for which the specificity for the intermediate snail host is very high will still succeed in infecting the snails, only if they are able to circumvent ROS by increasing their ROS scavenger production.

However, Nuismer et al. (2007, 2010) state that correlation could occur if interactions are mediated by a mechanism of phenotype matching such as what takes place for host-parasite interactions. This phenotype matching process was proposed for our *S. mansoni / B. glabrata* model of interest (Théron and Coustau, 2005).

Therefore whatever are the mechanisms involved in the apparition of trait correlation between two interacting species, our present results reveal the existence of phenotypic matching between host and parasitic strains in terms of their attack (ROS production) and defense (ROS scavenging) traits. To our knowledge, this work provides the first example of a clear link between the level of oxidant and antioxidant molecules possibly resulting from sympatric co-evolution, and provides supporting evidence for a field illustration of the Red Queen Hypothesis (Van Valen, 1974) and its predictions of a functional trait in a metazoan host/parasite model. Detailed mechanistic studies will be conducted in multiple populations to fully confirm the link between correlated traits and the Red Queen context.

**Acknowledgments**

We thank Bernard Dejean and Anne Rognon for technical assistance; Dr. Carole Blanchard for advice on measuring ROS levels in plasma; and Julien Portela for helping with the ROS titration experiments. The work received funding from the Schistophepigen (ANR-07-BLAN-0119-02) and BiomGenIm (ANR-07-BLAN-0214-03) programs of the French National Agency for Research, Centre National de la Recherche Scientifique, and Université de Perpignan Via Domitia. The funders had no role in the study design, data collection, data analysis, the decision to publish or manuscript preparation.

**References**

Bahia, D., Avelar, L., Mortara, R.A., Khayath, N., Yan, Y., Noel, C., Capron, M., Dissous, C., Pierce, R.J., Oliveira, G., 2006. SmPKC1, a new protein kinase C identified in the platyhelminth parasite *Schistosoma mansoni*. Biochem. Biophys. Res. Commun. 345, 1138-1148.

Bayne, C.J., 2009. Successful parasitism of vector snail *Biomphalaria glabrata* by the human blood fluke (trematode) *Schistosoma mansoni*: a 2009 assessment. Mol. Biochem. Parasitol. 165, 8-18.

586 Bayne, C.J., Hahn, U.K., Bender, R.C., 2001. Mechanisms of molluscan host resistance and of
587 parasite strategies for survival. Parasitology 123 Suppl, S159-167.
588 Bech, N., Beltran, S., Portela, J., Rognon, A., Allienne, J.F., Boissier, J., Theron, A., 2010. Follow-
589 up of the genetic diversity and snail infectivity of a *Schistosoma mansoni* strain from field to
590 laboratory. Infect. Genet. Evol. 10, 1039-1045.
591 Beltran, S., Boissier, J., 2008. Schistosome monogamy: who, how, and why? Trends Parasitol. 24,
592 386-391.
593 Beltran, S., Cezilly, F., Boissier, J., 2008. Genetic dissimilarity between mates, but not male
594 heterozygosity, influences divorce in schistosomes. PLoS ONE 3, e3328.
595 Bender, R.C., Broderick, E.J., Goodall, C.P., Bayne, C.J., 2005. Respiratory burst of *Biomphalaria*
596 *glabrata* hemocytes: *Schistosoma mansoni*-resistant snails produce more extracellular H2O2 than
597 susceptible snails. J. Parasitol. 91, 275-279.
598 Bender, R.C., Goodall, C.P., Blouin, M.S., Bayne, C.J., 2007. Variation in expression of
599 *Biomphalaria glabrata* SOD1: a potential controlling factor in susceptibility/resistance to
600 Schistosoma mansoni. Dev. Comp. Immunol. 31, 874-878.
601 Bernal, D., Carpena, I., Espert, A.M., De la Rubia, J.E., Esteban, J.G., Toledo, R., Marcilla, A.,
602 2006. Identification of proteins in excretory/secretory extracts of *Echinostoma friedi* (Trematoda)
603 from chronic and acute infections. Proteomics 6, 2835-2843.
604 Bienert, G.P., Schjoerring, J.K., Jahn, T.P., 2006. Membrane transport of hydrogen peroxide.
605 Biochim. Biophys. Acta 1758, 994-1003.
606 Bouchut, A., Roger, E., Gourbal, B., Grunau, C., Coustau, C., Mitta, G., 2008. The compatibility
607 polymorphism in invertebrate host/trematodes interactions: research of molecular determinants.
608 Parasite 15, 304-309.
609 Bouchut, A., Sautiere, P.E., Coustau, C., Mitta, G., 2006. Compatibility in the *Biomphalaria*
610 *glabrata/Echinostoma caproni* model: Potential involvement of proteins from hemocytes revealed
611 by a proteomic approach. Acta Trop. 98, 234-246.

612 Cass, C.L., Johnson, J.R., Califf, L.L., Xu, T., Hernandez, H.J., Stadecker, M.J., Yates, J.R., 3rd,
613 Williams, D.L., 2007. Proteomic analysis of *Schistosoma mansoni* egg secretions. Mol. Biochem.
614 Parasitol. 155, 84-93.
615 Chernin, E., 1963. Observations on hearts explanted in vitro from the snail Australorbis glabratus.
616 The Journal of parasitology 49, 353-364.
617 Combes, C., 2000. Selective pressure in host-parasite systems. J. Soc. Biol. 194, 19-23.
618 Curwen, R.S., Ashton, P.D., Johnston, D.A., Wilson, R.A., 2004. The *Schistosoma mansoni* soluble
619 proteome: a comparison across four life-cycle stages. Mol. Biochem. Parasitol. 138, 57-66.
620 Damian, R.T., 1997. Parasite immune evasion and exploitation: reflections and projections.
621 Parasitology 115 Suppl, S169-175.
622 de Jong-Brink, M., Bergamin-Sassen, M., Solis Soto, M., 2001. Multiple strategies of schistosomes
623 to meet their requirements in the intermediate snail host. Parasitology 123 Suppl, S129-141.
624 Dybdahl, M.F., Storfer, A., 2003. Parasite local adaptation: Red Queen versus Suicide King. Trends
625 in ecology & evolution 18, 523-530.
626 Dzik, J.M., 2006. Molecules released by helminth parasites involved in host colonization. Acta
627 Biochim. Pol. 53, 33-64.
628 Forde, S.E., Thompson, J.N., Bohannan, B.J., 2004. Adaptation varies through space and time in a
629 coevolving host-parasitoid interaction. Nature 431, 841-844.
630 Forde, S.E., Thompson, J.N., Holt, R.D., Bohannan, B.J., 2008. Coevolution drives temporal
631 changes in fitness and diversity across environments in a bacteria-bacteriophage interaction.
632 Evolution 62, 1830-1839.
633 Gagneux, S., DeRiemer, K., Van, T., Kato-Maeda, M., de Jong, B.C., Narayanan, S., Nicol, M.,
634 Niemann, S., Kremer, K., Gutierrez, M.C., Hilty, M., Hopewell, P.C., Small, P.M., 2006. Variable
635 host-pathogen compatibility in Mycobacterium tuberculosis. Proc. Natl. Acad. Sci. U. S. A. 103,
636 2869-2873.

637 Gasnier, N., Rondelaud, D., Abrous, M., Carreras, F., Boulard, C., Diez-Banos, P., Cabaret, J.,
638 2000. Allopatric combination of *Fasciola hepatica* and *Lymnaea truncatula* is more efficient than
639 sympatric ones. Int. J. Parasitol. 30, 573-578.
640 Gerard, C., Balzan, C., Theron, A., 1995. Spatial distribution patterns of the sporocyst
641 infrapopulation of *Schistosoma mansoni* within its mollusc host (*Biomphalaria glabrata*): an
642 unusual phenotype of aggregation. J. Parasitol. 81, 310-312.
643 Goodall, C.P., Bender, R.C., Broderick, E.J., Bayne, C.J., 2004. Constitutive differences in Cu/Zn
644 superoxide dismutase mRNA levels and activity in hemocytes of *Biomphalaria glabrata* (Mollusca)
645 that are either susceptible or resistant to *Schistosoma mansoni* (Trematoda). Mol. Biochem.
646 Parasitol. 137, 321-328.
647 Green, D.M., Kraaijeveld, A.R., Godfray, H.C., 2000. Evolutionary interactions between
648 *Drosophila melanogaster* and its parasitoid *Asobara tabida*. Heredity 85 Pt 5, 450-458.
649 Guillou, F., Mitta, G., Dissous, C., Pierce, R., Coustau, C., 2004. Use of individual polymorphism
650 to validate potential functional markers: case of a candidate lectin (BgSel) differentially expressed
651 in susceptible and resistant strains of *Biomphalaria glabrata*. Comp. Biochem. Physiol. B Biochem.
652 Mol. Biol. 138, 175-181.
653 Guillou, F., Roger, E., Moné, Y., Rognon, A., Grunau, C., Theron, A., Mitta, G., Coustau, C.,
654 Gourbal, B.E., 2007. Excretory-secretory proteome of larval *Schistosoma mansoni* and
655 *Echinostoma caproni*, two parasites of *Biomphalaria glabrata*. Mol. Biochem. Parasitol. 155, 45-
656 56.
657 Hahn, U.K., Bender, R.C., Bayne, C.J., 2000. Production of reactive oxygen species by hemocytes
658 of *Biomphalaria glabrata* : carbohydrate-specific stimulation. Dev. Comp. Immunol. 24, 531-541.
659 Hahn, U.K., Bender, R.C., Bayne, C.J., 2001a. Involvement of nitric oxide in killing of Schistosoma
660 mansoni sporocysts by hemocytes from resistant *Biomphalaria glabrata*. J. Parasitol. 87, 778-785.

661 Hahn, U.K., Bender, R.C., Bayne, C.J., 2001b. Killing of *Schistosoma mansoni* sporocysts by
662 hemocytes from resistant *Biomphalaria glabrata*: role of reactive oxygen species. The Journal of
663 parasitology 87, 292-299.
664 Howard, J.C., 1991. Immunology. Disease and evolution. Nature 352, 565-567.
665 Howard, J.C., Jack, R.S., 2007. Evolution of immunity and pathogens. Eur. J. Immunol. 37, 1721-
666 1723.
667 Janzen, D.H., 1980. When is it coevolution ? Evolution 34, 611-612.
668 Kim, S.M., Kang, J.H., 1997. Peroxidative activity of human Cu,Zn-superoxide dismutase. Mol.
669 Cells 7, 120-124.
670 Knudsen, G.M., Medzihradszky, K.F., Lim, K.C., Hansell, E., McKerrow, J.H., 2005. Proteomic
671 analysis of *Schistosoma mansoni* cercarial secretions. Mol. Cell. Proteomics 4, 1862-1875.
672 Koskella, B., Lively, C.M., 2007. Advice of the rose: experimental coevolution of a trematode
673 parasite and its snail host. Evolution 61, 152-159.
674 Little, T.J., Watt, K., Ebert, D., 2006. Parasite-host specificity: experimental studies on the basis of
675 parasite adaptation. Evolution 60, 31-38.
676 Lohse, K., Gutierrez, A., Kaltz, O., 2006. Experimental evolution of resistance in *Paramecium*
677 *caudatum* against the bacterial parasite *Holospora undulata*. Evolution 60, 1177-1186.
678 Loker, E.S., Adema, C.M., 1995. Schistosomes, Echinostomes and Snails: Comparative
679 Immunobiology. Parasitology today 11, 120-124.
680 Mei, H., LoVerde, P.T., 1997. *Schistosoma mansoni*: the developmental regulation and
681 immunolocalization of antioxidant enzymes. Exp. Parasitol. 86, 69-78.
682 Moné, Y., Gourbal, B., Duval, D., Du Pasquier, L., Kieffer-Jaquinod, S., Mitta, G., 2010a. A Large
683 Repertoire of Parasite Epitopes Matched by a Large Repertoire of Host Immune Receptors in an
684 Invertebrate Host/Parasite Model. PLoS Negl. Trop. Dis. 4, e813.
685 Moné, Y., Mitta, G., Duval, D., Gourbal, B.E., 2010b. Effect of amphotericin B on the infection
686 success of *Schistosoma mansoni* in *Biomphalaria glabrata*. Exp. Parasitol. 125, 70-75.

687 Morgan, A.D., Gandon, S., Buckling, A., 2005. The effect of migration on local adaptation in a
688 coevolving host-parasite system. Nature 437, 253-256.
689 Mourao, M.d.M., Dinguirard, N., Franco, G.R., Yoshino, T.P., 2009a. Role of the Endogenous
690 Antioxidant System in the Protection of *Schistosoma mansoni* Primary Sporocysts against
691 Exogenous Oxidative Stress. PLoS Negl. Trop. Dis. 3, e550.
692 Mourao, M.M., Dinguirard, N., Franco, G.R., Yoshino, T.P., 2009b. Phenotypic screen of early-
693 developing larvae of the blood fluke, *Schistosoma mansoni*, using RNA interference. PLoS Negl.
694 Trop. Dis. 3, e502.
695 Munoz-Antoli, C., Marin, A., Trelis, M., Toledo, R., Esteban, J.G., 2010. Sympatric and allopatric
696 experimental infections of the planorbid snail *Gyraulus chinensis* with miracidia of *Euparyphium*
697 *albuferensis* (Trematoda: Echinostomatidae). J. Helminthol., 1-5.
698 Nelder, J.A., Mead, R., 1965. A Simplex Method for Function Minimization. Comput. J. 7, 308-
699 313.
700 Nuismer, S.L., Gomulkiewicz, R., Ridenhour, B.J., 2010. When is correlation coevolution? Am.
701 Nat. 175, 525-537.
702 Nuismer, S.L., Ridenhour, B.J., Oswald, B.P., 2007. Antagonistic coevolution mediated by
703 phenotypic differences between quantitative traits. Evolution 61, 1823-1834.
704 Oter, O., Ribou, A.C., 2009. Quenching of long lifetime emitting fluorophores with paramagnetic
705 molecules. J Fluoresc 19, 389-397.
706 Perez-Sanchez, R., Ramajo-Hernandez, A., Ramajo-Martin, V., Oleaga, A., 2006. Proteomic
707 analysis of the tegument and excretory-secretory products of adult *Schistosoma bovis* worms.
708 Proteomics 6 Suppl 1, S226-236.
709 Rharass, T., Vigo, J., Salmon, J.M., Ribou, A.C., 2006. Variation of 1-pyrenebutyric acid
710 fluorescence lifetime in single living cells treated with molecules increasing or decreasing reactive
711 oxygen species levels. Anal. Biochem. 357, 1-8.

712 Ribou, A.C., Vigo, J., Kohen, E., Salmon, J.M., 2003. Microfluorometric study of oxygen
713 dependence of (1"-pyrene butyl)-2-rhodamine ester probe in mitochondria of living cells. J.
714 Photochem. Photobiol. B 70, 107-115.
715 Ribou, A.C., Vigo, J., Salmon, J.M., 2004. Lifetime of fluorescent pyrene butyric acid probe in
716 single living cells for measurement of oxygen fluctuation. Photochem. Photobiol. 80, 274-280.
717 Roger, E., Gourbal, B., Grunau, C., Pierce, R.J., Galinier, R., Mitta, G., 2008a. Expression analysis
718 of highly polymorphic mucin proteins (Sm PoMuc) from the parasite Schistosoma mansoni. Mol.
719 Biochem. Parasitol. 157, 217-227.
720 Roger, E., Grunau, C., Pierce, R.J., Hirai, H., Gourbal, B., Galinier, R., Emans, R., Cesari, I.M.,
721 Cosseau, C., Mitta, G., 2008b. Controlled chaos of polymorphic mucins in a metazoan parasite
722 (*Schistosoma mansoni*) interacting with its invertebrate host (*Biomphalaria glabrata*). PLoS Negl.
723 Trop. Dis. 2, e330.
724 Roger, E., Mitta, G., Mone, Y., Bouchut, A., Rognon, A., Grunau, C., Boissier, J., Theron, A.,
725 Gourbal, B.E., 2008c. Molecular determinants of compatibility polymorphism in the *Biomphalaria*
726 *glabrata/Schistosoma mansoni* model: New candidates identified by a global comparative
727 proteomics approach. Molecular and Biochemical Parasitology 157, 205-216.
728 Schulte, R.D., Makus, C., Hasert, B., Michiels, N.K., Schulenburg, H., 2010. Multiple reciprocal
729 adaptations and rapid genetic change upon experimental coevolution of an animal host and its
730 microbial parasite. Proceedings of the National Academy of Sciences 107, 7359-7364.
731 Selkirk, M.E., Smith, V.P., Thomas, G.R., Gounaris, K., 1998. Resistance of filarial nematode
732 parasites to oxidative stress. Int. J. Parasitol. 28, 1315-1332.
733 Shapiro, S.S., Wilk, M.B., 1965. An analysis of variance test for normality (complete samples).
734 Biometrika 52, 591-611.
735 Steinauer, M.L., 2009. The sex lives of parasites: investigating the mating system and mechanisms
736 of sexual selection of the human pathogen *Schistosoma mansoni*. Int. J. Parasitol. 39, 1157-1163.

737 Stern, O., Volmer, M., 1919. The extinction period of fluorescence. Physikalische Zeitschrift 20,
738 183-188.
739 Théron, A., Coustau, C., 2005. Are *Biomphalaria* snails resistant to *Schistosoma mansoni*? J.
740 Helminthol. 79, 187-191.
741 Théron, A., Coustau, C., Rognon, A., Gourbiere, S., Blouin, M.S., 2008. Effects of laboratory
742 culture on compatibility between snails and schistosomes. Parasitology 135, 1179-1188.
743 Théron, A., Pages, J.R., Rognon, A., 1997. *Schistosoma mansoni*: distribution patterns of miracidia
744 among *Biomphalaria glabrata* snail as related to host susceptibility and sporocyst regulatory
745 processes. Exp. Parasitol. 85, 1-9.
746 van Balkom, B.W.M., van Gestel, R.A., Brouwers, J.F.H.M., Krijgsveld, J., Tielens, A.G.M., Heck,
747 A.J.R., van Hellemond, J.J., 2005. Mass Spectrometric Analysis of the *Schistosoma mansoni*
748 Tegumental Sub-proteome. J. Proteome Res. 4, 958-966.
749 Van Valen, L., 1974. Molecular evolution as predicted by natural selection. Journal of Molecular
750 Evolution 3, 89-101.
751 Vermeire, J.J., Taft, A.S., Hoffmann, K.F., Fitzpatrick, J.M., Yoshino, T.P., 2006. *Schistosoma*
752 *mansoni*: DNA microarray gene expression profiling during the miracidium-to-mother sporocyst
753 transformation. Mol. Biochem. Parasitol. 147, 39-47.
754 Vermeire, J.J., Yoshino, T.P., 2007. Antioxidant gene expression and function in in vitro-
755 developing *Schistosoma mansoni* mother sporocysts: possible role in self-protection. Parasitology
756 134, 1369-1378.
757 Webster, J.P., Davies, C.M., 2001. Coevolution and compatibility in the snail-schistosome system.
758 Parasitology 123 Suppl, S41-56.
759 Webster, J.P., Gower, C.M., Blair, L., 2004. Do hosts and parasites coevolve? Empirical support
760 from the *Schistosoma system*. Am. Nat. 164 Suppl 5, S33-51.

761 Wu, X.J., Sabat, G., Brown, J.F., Zhang, M., Taft, A., Peterson, N., Harms, A., Yoshino, T.P., 2009.
762 Proteomic analysis of *Schistosoma mansoni* proteins released during in vitro miracidium-to-
763 sporocyst transformation. Mol. Biochem. Parasitol. 164, 32-44.
764 Yim, M.B., Chock, P.B., Stadtman, E.R., 1993. Enzyme function of copper, zinc superoxide
765 dismutase as a free radical generator. J. Biol. Chem. 268, 4099-4105.
766 Yim, M.B., Kang, J.H., Yim, H.S., Kwak, H.S., Chock, P.B., Stadtman, E.R., 1996. A gain-of-
767 function of an amyotrophic lateral sclerosis-associated Cu,Zn-superoxide dismutase mutant: An
768 enhancement of free radical formation due to a decrease in Km for hydrogen peroxide. Proc. Natl.
769 Acad. Sci. U. S. A. 93, 5709-5714.
770 Yoder, J.B., Nuismer, S.L., 2010. When does coevolution promote diversification? Am. Nat. 176,
771 802-817.
772 Zelck, U.E., Von Janowsky, B., 2004. Antioxidant enzymes in intramolluscan *Schistosoma mansoni*
773 and ROS-induced changes in expression. Parasitology 128, 493-501.
774
775

## Figure legends

**Fig. 1.** Effect of hydrogen peroxide ($H_2O_2$) on *Schistosoma mansoni* sporocysts. (A) Cytotoxicity among *S. mansoni* sporocysts 2 h after exposure to different $H_2O_2$ concentrations. The asterisk indicates a significant difference ($P < 0.05$) in the cytotoxic effect of $H_2O_2$ on *S. mansoni* Guadeloupean strain (*Sm*GH2) versus *S. mansoni* Brazilian strain (*Sm*BRE) sporocysts. (B) Percent sporocyst mortality after 4 h exposure to different $H_2O_2$ concentrations. The asterisk indicates a significant difference ($P < 0.05$) in the mortality rates of *Sm*GH2 versus *Sm*BRE sporocysts.

**Fig. 2.** Constitutive total antioxidant capacities of *Schistosoma mansoni* Guadeloupean strain (*Sm*GH2) and *S. mansoni* Brazilian strain (*Sm*BRE) sporocysts. Values are expressed as µM of antioxidant activity per 10 µg of sporocyst proteins. The asterisk indicates a significant difference ($P < 0.05$).

**Fig. 3.** Ratios of Zn-Cu superoxide dismutase (Zn-Cu SOD, Smp_176200.2) transcript levels in the two strains of *Schistosoma mansoni* miracidia (Guadeloupean strain, *Sm*GH2 and Brazilian strain, *Sm*BRE). Ratios were determined using real-time quantitative PCR and are expressed relative to the expression levels of 28s rRNA and α-tubulin. The histogram represents the average values of duplicates ± S.D. The expression ratio was calculated according to the formula: $R = 2(\Delta Ct)$, where $\Delta Ct$ represents Ct (target gene) – Ct (constitutively expressed gene).

**Fig. 4.** Intracellular ROS measurements in single *Biomphalaria glabrata* hemocytes (A) Global reactive oxygen species (ROS) concentration in each snail strain. The histogram represents the ROS concentrations in arbitrary units (-fold mean) for the *Biomphalaria glabrata* Guadeloupean strain, *Bg*GUA and Brazilian strain, *Bg*BRE. The asterisk indicates a significant difference ($P < 0.05$) in ROS production by hemocytes of the two snail strains. (B) ROS concentrations in hemocyte populations from *Bg*GUA and *Bg*BRE snails. The histograms represent the fluorescent lifetimes of 1-pyrenebutyric acid (PBA)-loaded hemocytes from eight each of *Bg*GUA and *Bg*BRE; 108 single hemocytes from eight *Bg*BRE and 111 hemocytes from eight individuals of *Bg*GUA snails were assessed. The *x* axis represents the fluorescent lifetime in nanoseconds, while the *y* axis corresponds to the number of cells.

**Fig. 5.** Hydrogen peroxide ($H_2O_2$) production by *Biomphalaria glabrata* hemocytes. Cumulative production of $H_2O_2$ was measured using Amplex Red. The data are presented as the mean (± S.D.) of Amplex Red absorbance at 570 nm ($A_{570nm}$) per 45,000 cells over five replicates. The asterisk indicates a significant difference ($P < 0.05$) in $H_2O_2$ production from hemocytes of *B. glabrata* Guadeloupean strain, *Bg*GUA, versus Brazilian strain, *Bg*BRE.

**Fig. 6.** Constitutive superoxide anion plasma content in *Biomphalaria glabrata* Guadeloupean strain, *Bg*GUA, versus Brazilian strain, *Bg*BRE. The superoxide anion plasma content was assessed by spectrophotometric measurement (620 nm) of nitroblue tetrazolium (NBT) reduction. At 3 h after initiation of the reaction, the BgBRE plasma contained significantly more superoxide anion than that from *Bg*GUA (the asterisk indicates a significant difference; $P < 0.05$).

**Fig. 7.** Infection rates and intensities in sympatric and allopatric *Schistosoma mansoni/Biomphalaria glabrata* combinations. The percentage of snails infected and the intensity of infection: number of mother sporocysts (SpI) developed (*n* SpI) was measured after individual snails were challenged with different miracidial doses (1, 10, 20, 30 or 50 miracidia (Mi)).

**Fig. 8.** Schematic representation of our reactive oxygen species (ROS)-based co-evolutionary hypothesis. The percentage of prevalence is indicated for each *Biomphalaria glabrata*/*Schistosoma mansoni* combination. The number of arrows represents the differential host oxidant (ROS) or parasite antioxidant (ROS scavenger) capabilities. *Biomphalaria glabrata* Brazilian strain, *Bg*BRE, and Guadeloupean strain, *Bg*GUA; *S. mansoni* Brazilian strain, *Sm*BRE, and Guadeloupean strain, *Sm*GH2.

**Table 1**
Primer sequences for *Reverse Transcription-quantitative PCR* in this study.

| Gene Name and SchistoDB ID | Amplicon Length | Smp_scaffold | Forward primer (5' to 3') |
|---|---|---|---|
| Glyceraldehyde-3-phosphate dehydrogenase (GAPDH) Smp_056970 | 125 | 000155 | TGGCCGTGGAGCGATGCAAA |
| Glutathione S-transferase omega Smp_152710 | 148 | 000154 | ACAGCTCTAGTTGTCGACCAAACA |
| Glutathione S-transferase 28 kD (GST 28) Smp_054160 | 128 | 000143 | CGGACGCGGACGTGCTGAAT |
| Glutathione-S-transferase 26 kD (GST 26) Smp_163610 | 104 | 000249 | GCAAAGCTGGTGGTTTGGGGC |
| Glyoxalase II Smp_091010 | 124 | 000428 | ATGGCCTTCATTGCTTTGGACAGA |
| Thioredoxin peroxidase (TPX) Smp_158110 | 101 | | CAAAGGCCTTGTACAACCAACTC |
| Superoxide dismutase (SOD) Smp_176200.2 | 100 | 000615 | AGTGGACTCAAGGCTG |

Gene names are given according to the SchistoDB accession numbers (http://schistodb.net/schistodb20/). Their respective scaffolds are included in the table. Smp_163610 primer sequences are given according to the mRNA sequence of the gene (XM_002582157.1) due to inconsistency in the genome assembly. α-tubulin and 28S primers sequences were previously published (Bahia et al., 2006; Roger et al., 2008a).

**A**

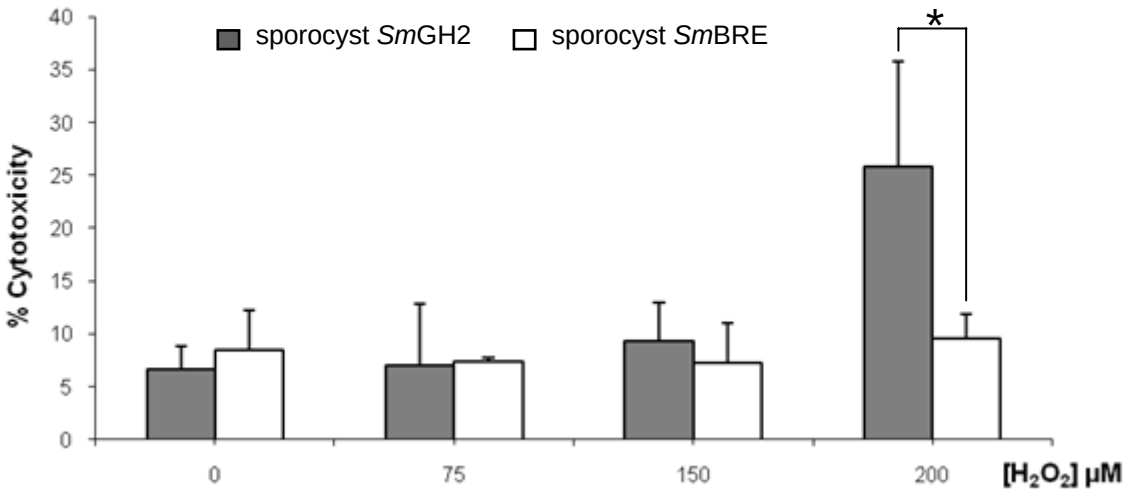
sporocyst *Sm*GH2
sporocyst *Sm*BRE
*
% Cytotoxicity
40
35
30
25
20
15
10
5
0
0
75
150
200
[H2O2] µM

**B**

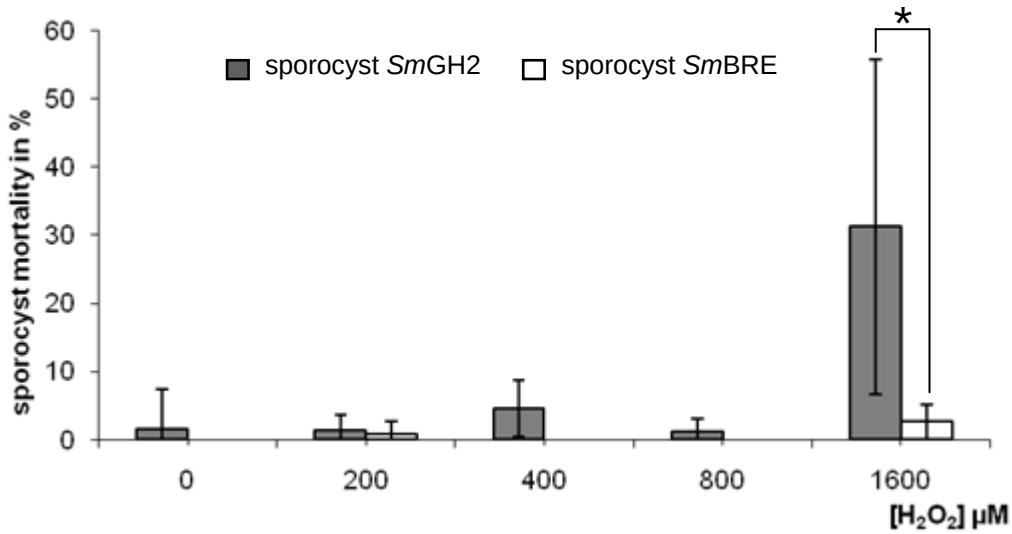
sporocyst *Sm*GH2
sporocyst *Sm*BRE
*
sporocyst mortality in %
60
50
40
30
20
10
0
0
200
400
800
1600
[H2O2] µM

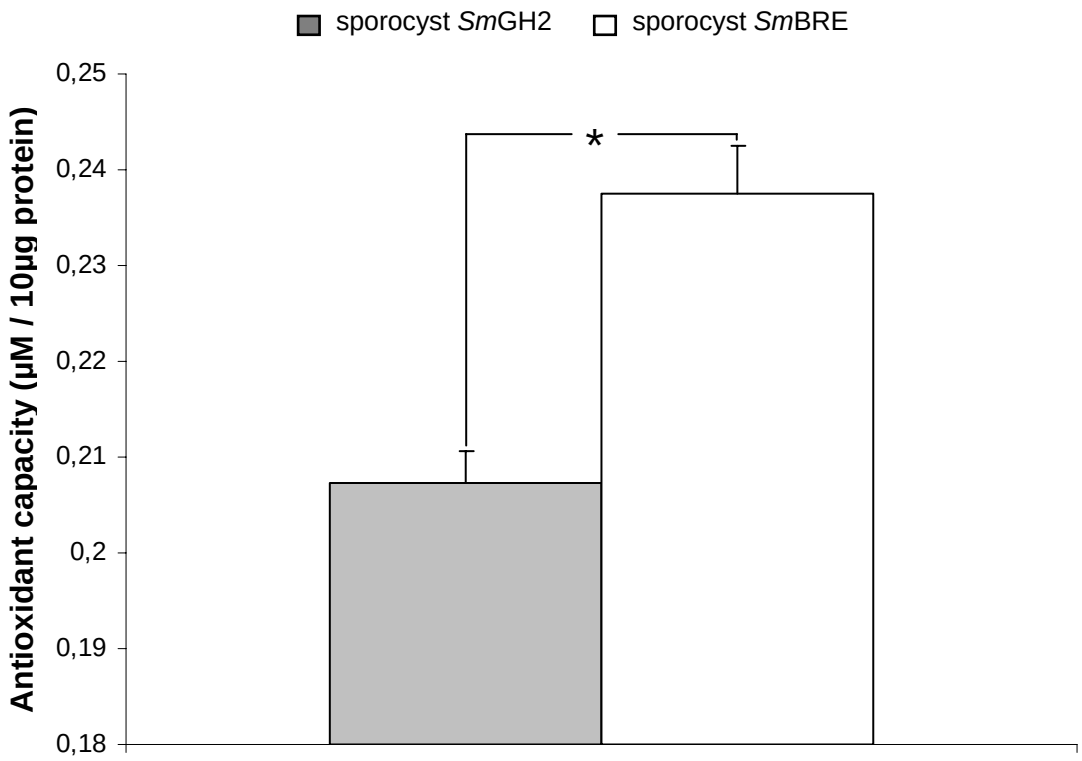
sporocyst SmGH2
sporocyst SmBRE
Antioxidant capacity (µM / 10µg protein)
0,25
0,24
0,23
0,22
0,21
0,2
0,19
0,18
*

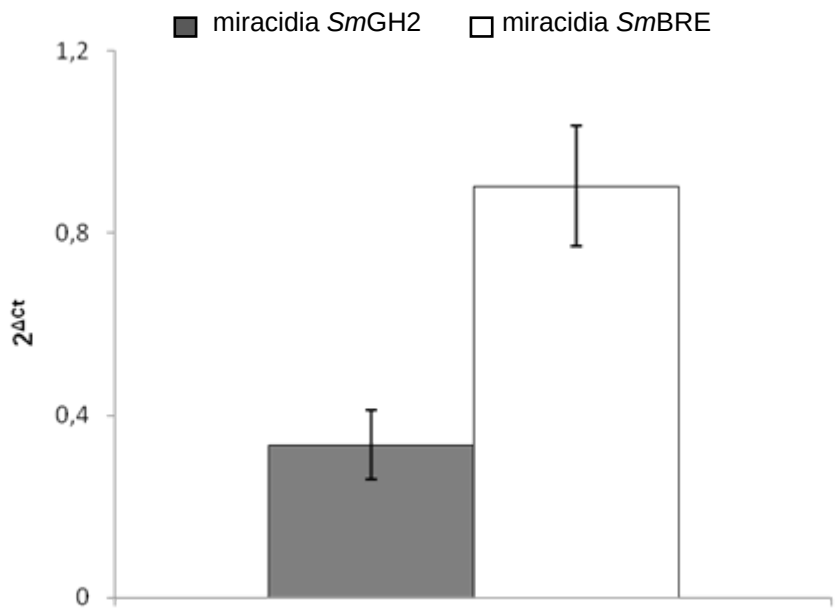
miracidia SmGH2
miracidia SmBRE
1,2
0,8
0,4
0
2Δct

**A**

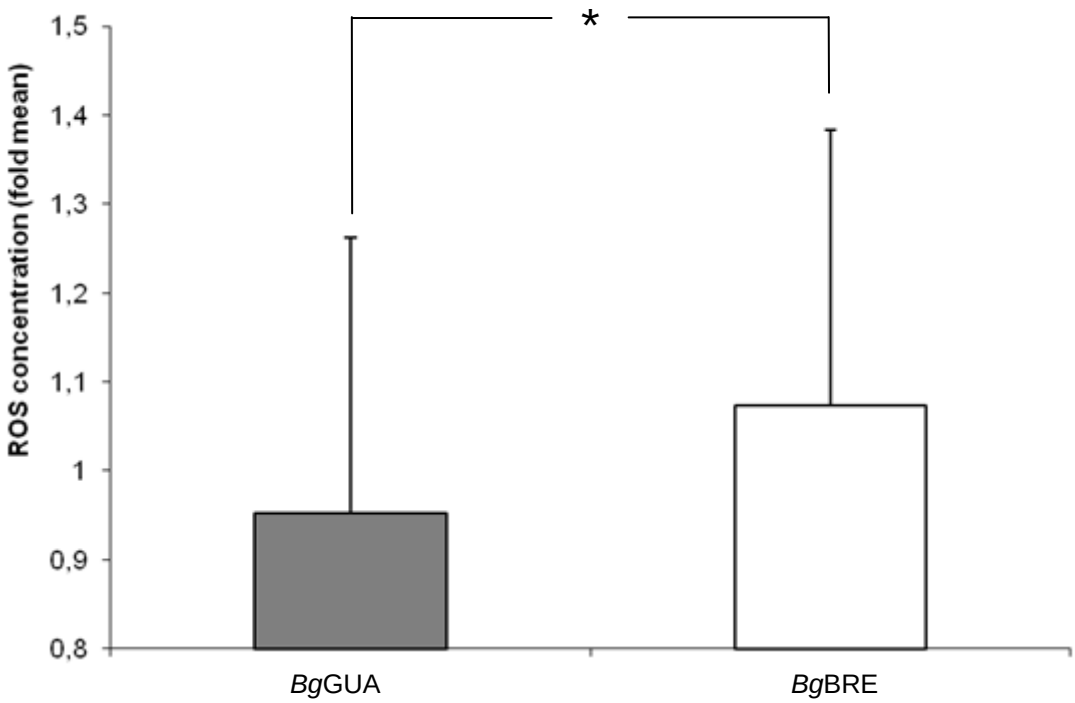
*
ROS concentration (fold mean)
1,5
1,4
1,3
1,2
1,1
1
0,9
0,8
BgGUA
BgBRE

**B**

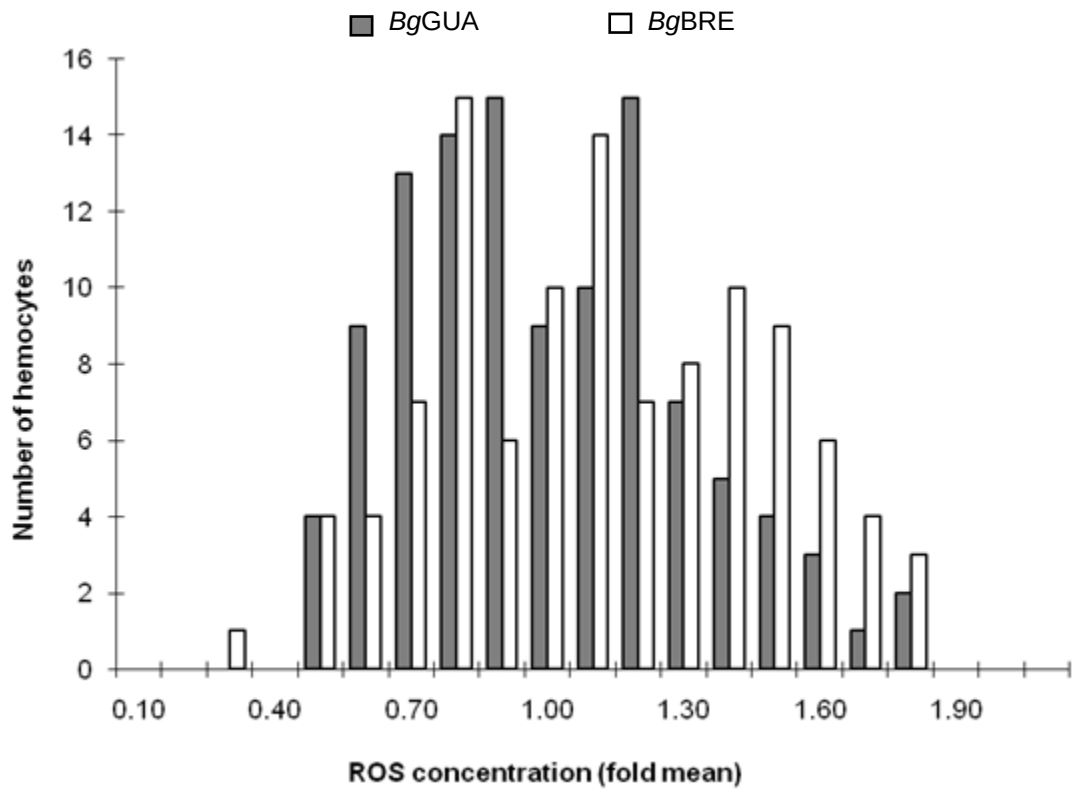
BgGUA
BgBRE
Number of hemocytes
16
14
12
10
8
6
4
2
0
0.10
0.40
0.70
1.00
1.30
1.60
1.90
ROS concentration (fold mean)

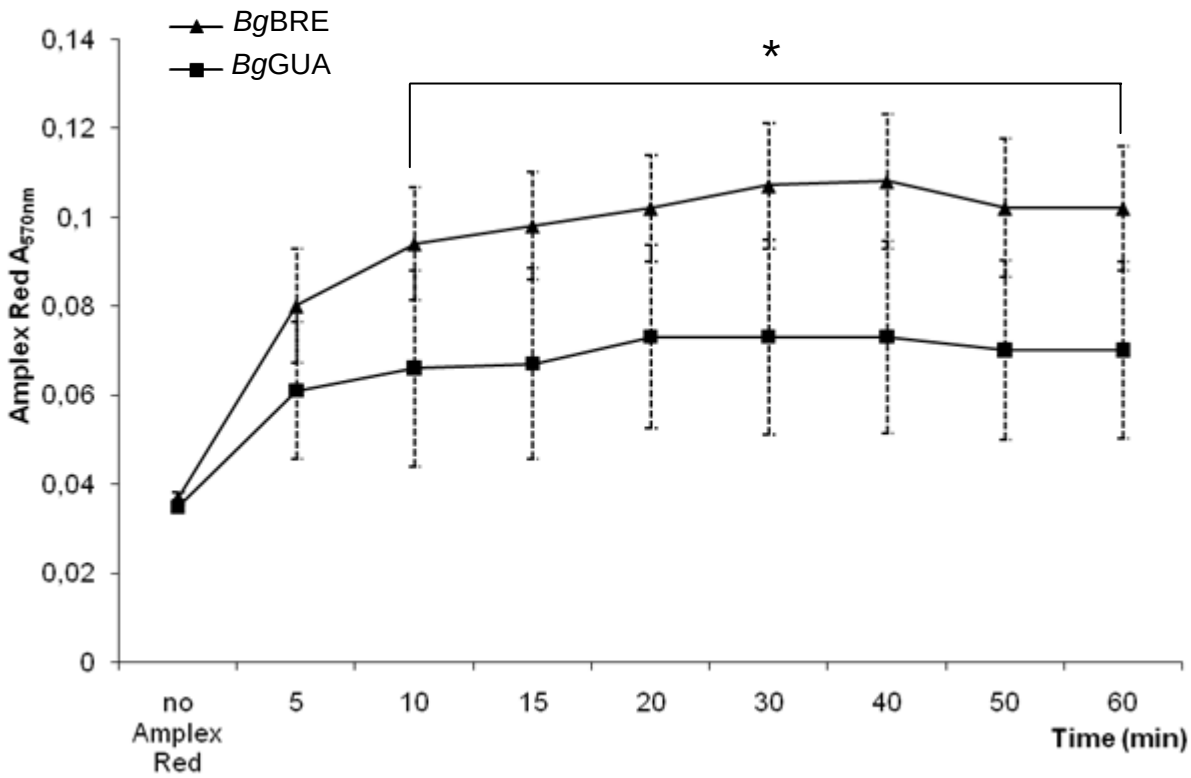
*Bg*BRE
*Bg*GUA
*
0,14
0,12
0,1
0,08
0,06
0,04
0,02
0
Amplex Red $A_{570nm}$
no Amplex Red
5
10
15
20
30
40
50
60
Time (min)

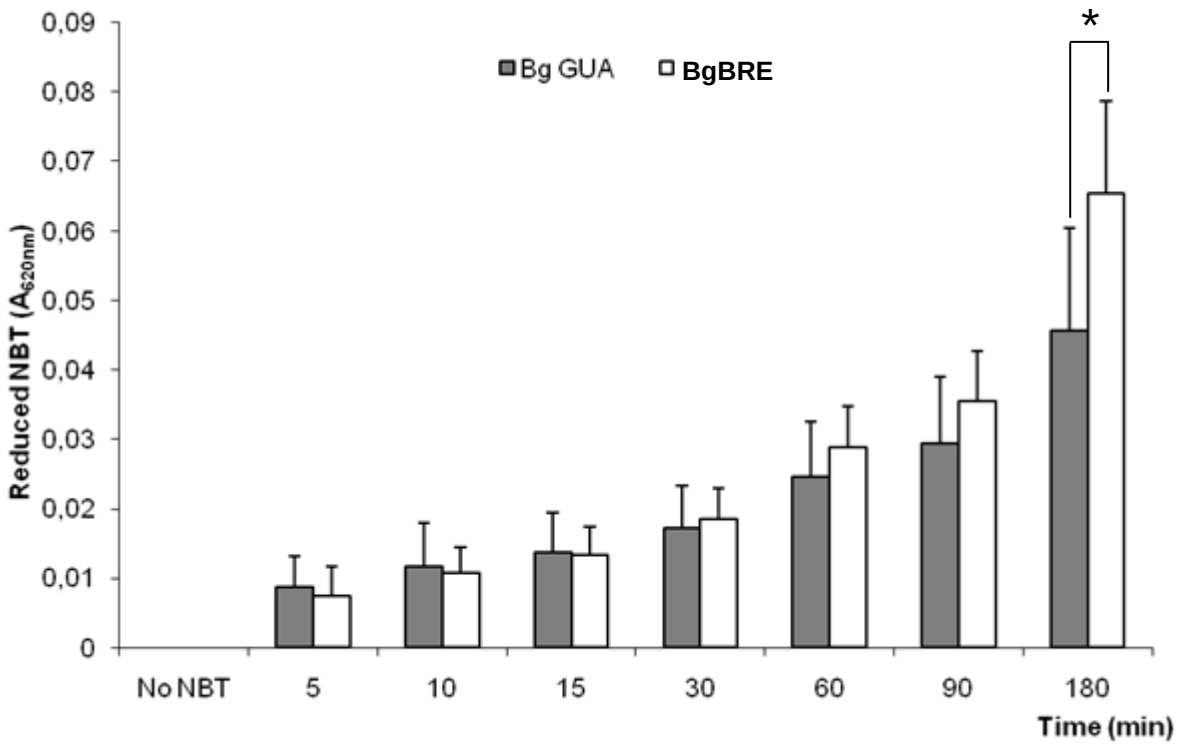
0,09
0,08
0,07
0,06
0,05
0,04
0,03
0,02
0,01
0
Reduced NBT (A620nm)
Bg GUA
BgBRE
*
No NBT
5
10
15
30
60
90
180
Time (min)

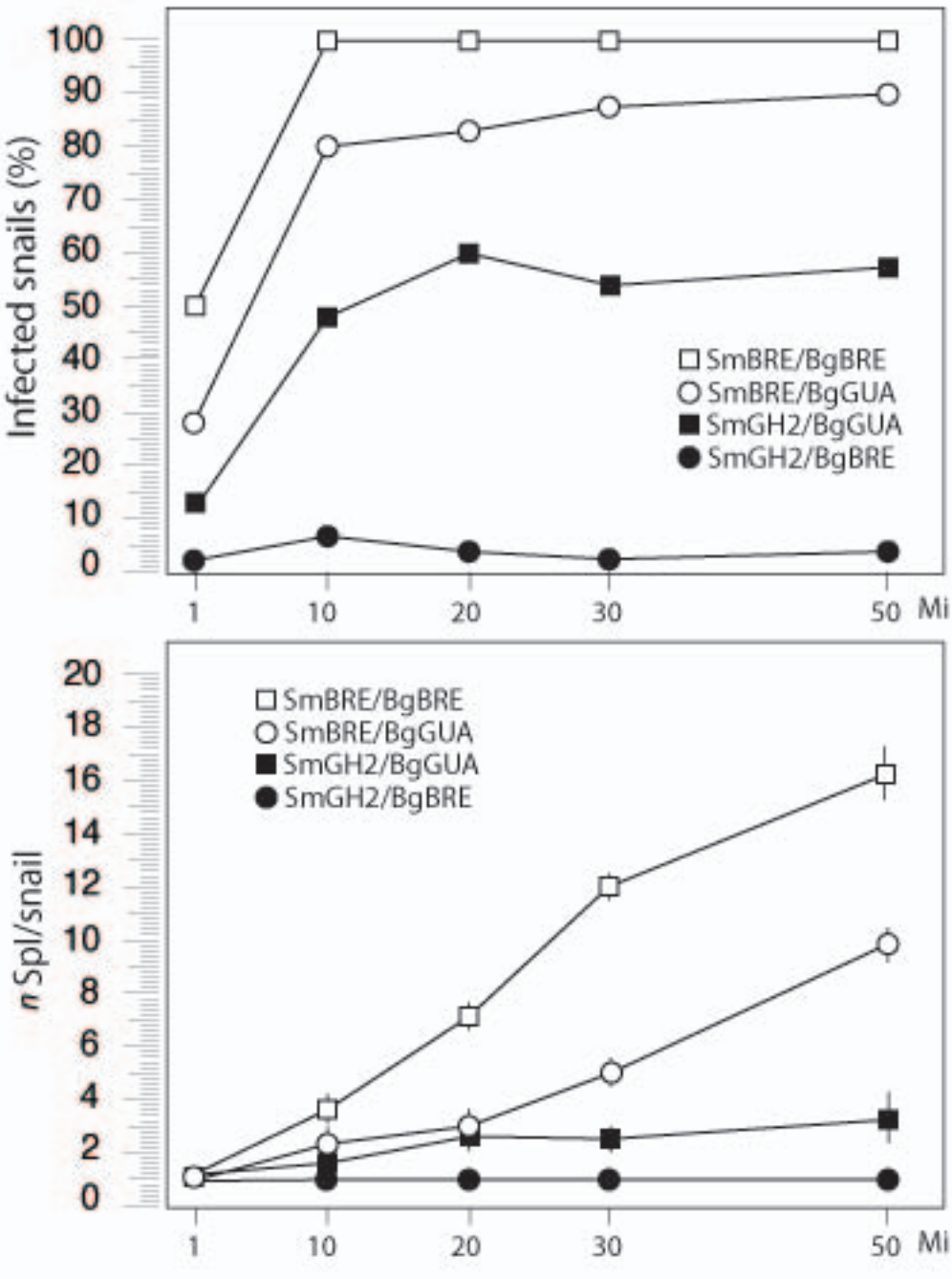
Infected snails (%)
100
90
80
70
60
50
40
30
20
10
0
1
10
20
30
50
Mi
SmBRE/BgBRE
SmBRE/BgGUA
SmGH2/BgGUA
SmGH2/BgBRE
n Spl/snail
20
18
16
14
12
10
8
6
4
2
0
1
10
20
30
50
Mi
SmBRE/BgBRE
SmBRE/BgGUA
SmGH2/BgGUA
SmGH2/BgBRE

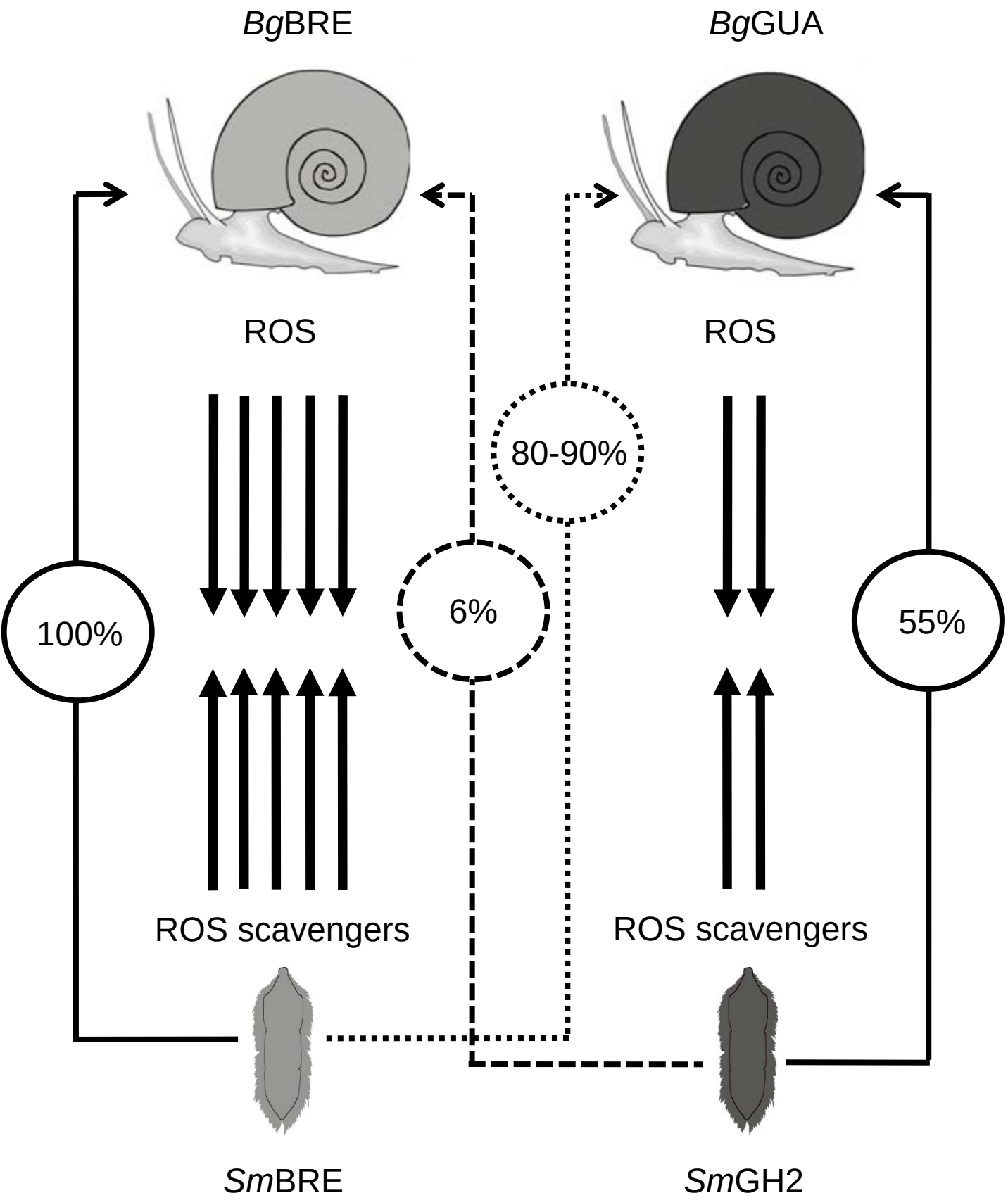
*Bg*BRE
*Bg*GUA
ROS
ROS
80-90%
6%
100%
55%
ROS scavengers
ROS scavengers
*Sm*BRE
*Sm*GH2